Ecological Engineering 112 (2018) 41–50

Contents lists available at ScienceDirect

Ecological Engineering

journal homepage: www.elsevier.com/locate/ecoleng

Evaluation of semiarid grassland degradation in North China from multiple perspectives

Dongmei Han[a], Guoqiang Wang[a,*], Baolin Xue[a], Tingxi Liu[b], Yinglan A[a], Xinyi Xu[a]

[a] College of Water Sciences, Beijing Normal University, Beijing 100875, China
[b] College of Water Conservancy and Civil Engineering, Inner Mongolia Agricultural University, Hohhot, Inner Mongolia Autonomous Region 010018, China

ARTICLE INFO

Keywords:
Grassland degradation
Multiple perspectives
AGB
Desertification
Species composition
Driving factors

ABSTRACT

There has been increasing interest in grassland ecosystem degradation resulting from intensive human activity and climate change, especially in arid and semiarid regions. Species composition, grassland desertification, and aboveground biomass (AGB) are used as indicators of grassland degradation. In this study, we comprehensively analyzed variations in these three indicators of grassland degradation in semiarid grassland in North China, on multiple time scales. Since 1984, species composition has become simpler and species indicative of grassland degradation, such as *Potentilla acaulis* and *Artemisia frigida*, have become dominant. These changes indicate that serious grassland degradation has occurred since 1984. Grassland degradation was also analyzed on shorter time scales. Analyses of interannual variations during 2005–2015 showed that desertification decreased and average AGB in the growing season increased over the study area, indicating that grassland was recovering. However, analyses of species composition indicated that grassland was actually degrading during this period. Analyses of spatial variations showed that the position of slightly desertified grassland shifted and formed a band in the west, where the lowest AGB in the growing season was recorded. Grassland AGB decreased in most parts of the south and east ($\sim 20\ g/m^2$ per decade) but increased in other regions from 2005 to 2015. Climatic factors had critical effects on grassland degradation, showing that simpler species composition mainly resulted from an increase in average temperature and a decrease in average precipitation over the past 30 years. And in recent decade, increased precipitation and decreases both in temperature and potential evapotranspiration relieved desertification and increased AGB overall. This study thus revealed that ecosystem structure degenerated seriously in the long-term, but AGB increased in the short-term mainly due to increases in both indicator species for grassland degradation and species with strong resistance to drought tolerance. Thus, this study suggested there had distinct difference in grassland degradation identified by above three indicators at different time-scales, and multiple perspectives should be considered to accurately assess the state and characteristics of grassland degradation.

1. Introduction

Natural grasslands cover $4 \times 10^8\ hm^2$ worldwide, accounting for 13% of the world's grassland area and 41% of the whole area of China. Almost 80% of the grassland in China is in arid and semiarid regions (Kang et al., 2007). Grassland is the largest terrestrial ecosystem in China and it has a high ecological and economic value. It plays a critical role in regional climates, biodiversity, conservation, provision of ecosystem services and socioeconomic development, and is also the main target of eco-environmental conservation, especially in Beijing-Tianjin-Hebei regions (Wu et al., 2014; Zhao et al., 2015). Numerous studies have shown that various grasslands in China have seriously degraded under long-term overgrazing and human disturbance (Li et al., 2015; Sarula et al., 2013; Wang et al., 2015). The continual degradation of grasslands has caused a series of problems, including grassland desertification, biodiversity loss, and the loss of carbon sinks. These problems threaten animal husbandry, ecological security, and sustainable development in China (Man et al., 2016).

Although many recent studies have focused on the indicators which are used to define grassland degradation, there is still debated regarding definition of grassland degradation at different temporal and spatial scales. Generally, decreases in both grassland biomass and vegetation coverage have been used to explain the degeneration of ecosystem function (Zhang et al., 2011; Wang et al., 2014). However, these estimates are far from comprehensive since they make no consideration of ecosystem structure. Also, several studies have suggested that species composition does not change during the transition stage of thicketization of grasslands, because the intensive interaction between shrub

* Corresponding author at: College of Water Sciences, Beijing Normal University, Xinjiekouwai Street 19, Haidian, Beijing 100875, China.
E-mail address: wanggq@bnu.edu.cn (G. Wang).

https://doi.org/10.1016/j.ecoleng.2017.12.011
Received 17 August 2017; Received in revised form 2 November 2017; Accepted 15 December 2017
Available online 04 January 2018
0925-8574/ © 2017 Elsevier B.V. All rights reserved.

patches and grass patches maintains biomass and diversity at low levels in an unstable ecosystem (Peng et al., 2013). Therefore, there are two main gaps in previous findings, one was the research on grassland degradation in semiarid grassland of North China is insufficient and weak, and the other was that one simple perspective or single indicator is inaccurate to estimate grassland degradation. Moreover, the patterns of grassland degradation are distinctive between the long-term and short-term scales.

To address in-depth analyses from multiple perspectives to explore the characteristics of grassland degradation accurately and comprehensively, these three indicators including species composition, desertification and aboveground biomass (AGB), are considered at the inter-decades, inter-annual, and intra-annual scales, respectively. Thus, the main objectives of this study were (a) to evaluate the accuracy of AGB, grassland desertification, and dominant species composition as indicators of grassland degradation on different temporal and spatial scales, respectively, (b) to discuss the differences and similarities among these indicators of grassland degradation, and (c) to explore the potential driving factors for changes in these indicators on multiple scales.

2. Materials and methods

2.1. Study area description

The study area, located in the northeast of North China's Inner Mongolia, is a transition zone from mountains to high plains (Fig. 1). Its terrain slopes from southeast to northwest with altitudes of 600–800 m above sea level. This area experiences a temperate continental monsoon climate. According to meteorological observation for many years, the annual mean precipitation is approximately 300–500 mm, and annual average temperature is −2.4 to −2.2 °C. The growing season is generally from May to September when 80% of annual precipitation occurs and the mean temperature is 19.7–37.7 °C. The main vegetation types are meadow steppe and montane forest steppe (including forest steppe and grassland). And the dominant plant species are *Leymus chinensis* (*L.chinensis*), *Stipa baicalensis* (*S. baicalensis*), and *Cleistogenes squarrosa* (*C. squarrosa*) over study area. According to field surveys, the productivity and diversity of the grassland ecosystem has declined dramatically in recent years. The natural grassland covering 81.2% of total land area, whereas the areas of degraded grassland and desertification is accounting for nearly 53% of natural grassland. Meanwhile, grassland degradation has affected the distribution of temperature, water, and physicochemical properties of soil in this study area (Li et al., 2015; Wang et al., 2015; Wang et al., 2017).

2.2. Sampling and meteorological data preparation

Two field datasets were used to investigate the vegetation community during the peak growing period of semiarid grassland in North China. One dataset was from 75 plots (1 m × 1 m) sampled from July 11 to July 24, 2015. The other dataset was from 55 randomly selected plots (1 m × 1 m) sampled from July 27 to August 8, 2016. The survey parameters recorded in each plot were amount, coverage, height, and density of all plants, height and coverage of plant communities, and location (longitude, latitude, and altitude). The AGB were clipped at ground level in the two random 0.25m^2 quadrats within each plot, and then dried to constant weight at 60 °C before measuring dry weight (Coyle et al., 2008). In all quadrats, vegetation coverage was measured by the cable method (Ren, 1998).

Monthly precipitation, temperature, and other climatic factors (wind speed at 10-m height, sunshine duration, and relative humidity) in and around the study region were recorded at four meteorological stations of the China Meteorological Data Service Center (CMDC) from

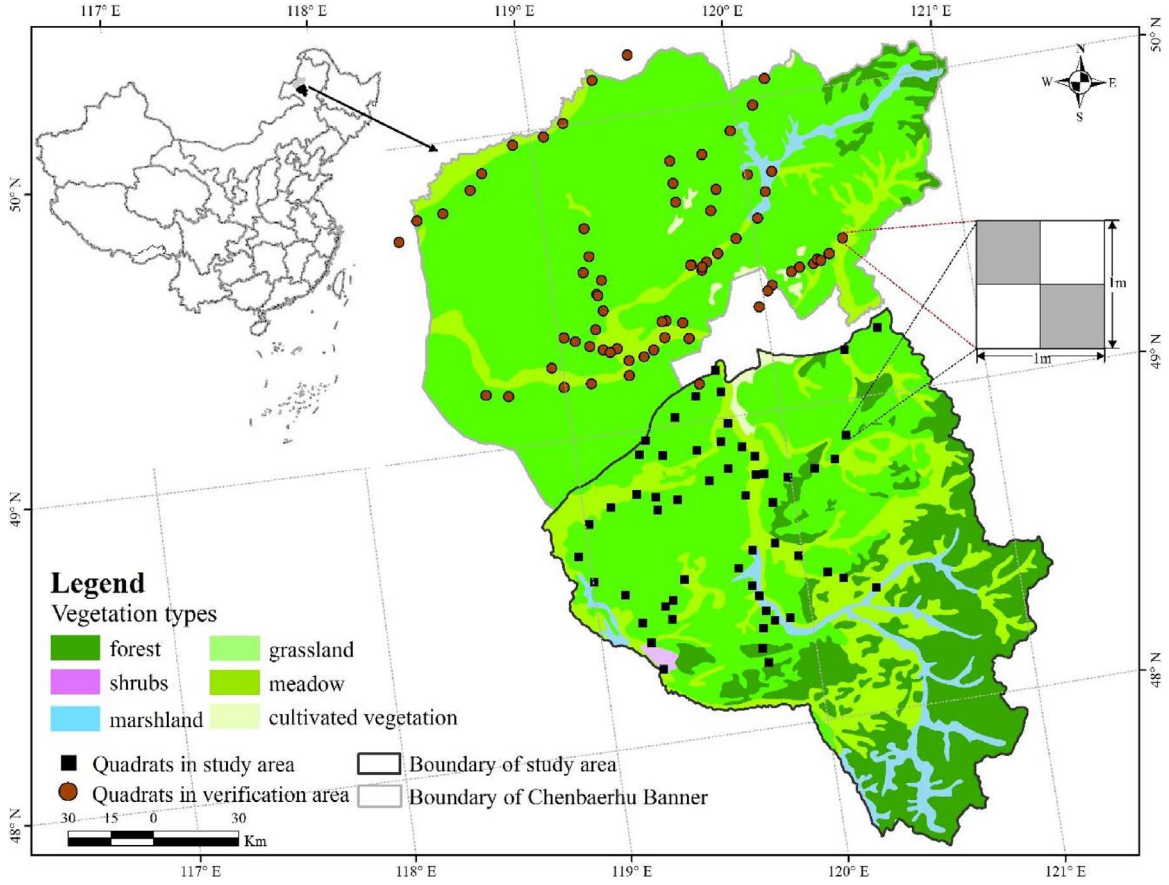

Fig. 1. Spatial distribution of sampling sites and vegetation types in the study area.

1980 to 2015. Spatial interpolation techniques were used to match the spatial distributions of precipitation, temperature, and potential evapotranspiration (PET) using the Kriging method. Average precipitation, temperature, and PET in the growing season were calculated over the study area from May to September. Annual precipitation and temperature were calculated from January to December.

2.3. Acquisition of satellite remote sensing data

A normalized difference vegetation index (NDVI) time-series of satellite-based images (250 mm spatial and 16-day temporal resolution; MODerate Resolution Imaging Spectroradiometer, MODIS), covering the period from May to September in 2005–2016, was obtained from https://modis.gsfc.nasa.gov/data/dataprod/mod13.php. The MODIS tiles, including h25v03, h25v04, h26v03, and h26v04, were mosaicked and redefined to an Albers projection. The NDVI images of the study area were clipped from the mosaicked tiles. Monthly NDVI images corresponding to sampling data were extracted to average two 16-day NDVIs in the current month, and the average NDVI in the growing season was obtained using the maximum value composite (MVC) of May to September (Holben, 1986). MODIS can provide continuous information for vegetation to cover a lack of field data at various spatial and temporal scales (Amarnath et al., 2017; Carroll et al., 2010).

We extracted the distribution map of species composition in 1984 over study area. To identify changes in species composition between 2016 (experimental year) and 1984, the partitions of species composition in 2016 were compared with those in 1984.

2.4. Determination of dominant species by sample plot index (SPI)

The sample plot index (SPI) reflected dominant species more effectively than simple importance value (SIV), which did not show a good fit for species classification (He, 2004). The SPI explained vegetation dominance by comparing one species with other species in the same sample plot, and with the same species among all sample plots. The SPI was calculated as follows:

$$\mathrm{SPI}_i = \frac{300 \times m \times (H_i C_i)^2}{\sum_i^n (H_i C_i) \times \sum_j^m (H_{ij} C_{ij})}, \tag{1}$$

where, SPI_i represents sample plot index of *i* species in one sample plot in the study area, *i* represents species, *j* represents sample plot, *n* represents number of species in one sample plot, *m* represents number of sample plots number where *i* species existed, *Hi* represents average height of *i* species in one sample plot (in cm or m); *Hij* represents average height of *i* species in *j* sample plot (in cm or m); *Ci* represents coverage area of *i* species in one sample plot (in cm^2 or m^2); and *Cij* represents coverage area of *i* species in *j* sample plot (in cm^2 or m^2).

2.5. Definition of various grassland desertification

Grassland desertification, also known as grassland sandy desertification, is the main component of grassland degradation. Monitoring is generally periodic to analyze dynamic changes of grassland desertification every year. Therefore, with reference to the Chinese national standard "Parameters for degradation, sandification, and salification of rangelands" (GB19377-2003), and to other relevant research on the grades of desertification, we established the grades of grassland desertification by combining sampling data, the grassland type, and the environmental conditions in the study area (Table 1).

Some studies have indicated that there is an extremely significant linear relationship between vegetation coverage and NDVI in Chinese grassland (Qin et al., 2008; Huo et al., 2008). Thus, surface vegetation coverage can be obtained by constructing a linear relationship model with NDVI (Eq. (2)):

Table 1
Remote sensing gradation criteria of grassland sandy desertification.

Desertification degree	Vegetation coverage	Performance
Non- desertified grassland (Non-DG)	> 70%	desertified land with good crop growth
Slightly desertified grassland (SlD)	50%–70%	desertified land normal crop growth, without sand-moving
Moderately desertified grassland (MD)	30%–50%	no sand-moving, low crop growth
Severely desertified grassland (SeD)	< 30%	obvious crop growth, wind erosion gobi, poor crop growth

$$V_C = \frac{NDVI - NDVI_S}{NDVI_V - NDVI_S} \times 100\%, \tag{2}$$

where, $V_C$represents vegetation coverage, $NDVI_S$ represents the minimum NDVI in study area (bare soil), and $NDVI_V$ represents the maximum NDVI (pure vegetation pixel).

2.6. Establishment and validation of AGB inversion model

By comparison among NDVI, EVI, and RVI, there had a high relationship between NDVI and AGB (Todd et al., 1998; Li and Jian, 2004; Li et al., 2007). Thus, we established three simple functions between NDVI and AGB (linear, power, and logarithmic functions). The performance of the models was assessed by the root mean squared error (RMSE), the correlation coefficient (R), and relative error (RE). The functions to estimate grassland AGB were as follows:

$$AGB_{grassland} = f_{AGB}(NDVI), \tag{3}$$

$$AGB_{grassland} = \mathrm{a} \times NDVI + b, \tag{4}$$

$$AGB_{grassland} = c \times NDVI^d, \tag{5}$$

$$AGB_{grassland} = m \times \ln(NDVI) + k, \tag{6}$$

where $AGB_{grassland}$ represents the grassland aboveground biomass, $f_{AGB}(NDVI)$ represents the function to estimate AGB, and a, b, c, d, m, and k represent the coefficients of the three functions.

The criteria used to assess the models were calculated as follows:

$$\mathrm{r} = \frac{\left(n\sum_{i=1}^n NDVI_i AGB_{grassland\,i} - \sum_{i=1}^n NDVI_i \cdot \sum_{i=1}^n AGB_{grassland\,i}\right)}{\left(\sqrt{n\sum_{i=1}^n NDVI_i{}^2 - \left(\sum_{i=1}^n NDVI_i\right)^2} \cdot \sqrt{n\cdot\sum_{i=1}^n AGB_{grassland\,i}{}^2 - \left(\sum_{i=1}^n AGB_{grassland\,i}\right)^2}\right)}, \tag{7}$$

$$\mathrm{RMSE} = \sqrt{\frac{1}{n}\sum_{i=1}^n (AGB_{grassland\,i} - AGB_{grassland\,i}')^2}, \tag{8}$$

$$\mathrm{RE} = \frac{\sum_{i=1}^n (|AGB_{grassland\,i}' - AGB_{grassland\,i}|/AGB_{grassland\,i})}{n} \times 100\%, \tag{9}$$

where $NDVI_i$ represents the NDVI value corresponding to i^{th} sample, $AGB_{grasslandi}$ is the i^{th} observed sampling data, $AGB_{grassland\,i}'$ is the i^{th} simulated data, and *n* is the total number of the validation set.

Two experimental datasets were selected to analyze the applicability of AGB retrieval models, with an emphasis on the ability of each model to estimate AGB on different temporal and spatial scales. Sampling data in 2016 were selected as the calibration set to estimate the parameters to build the model. Sampling data in 2015 were used as the validation set to test the models. Then, r, RMSE, and RE were

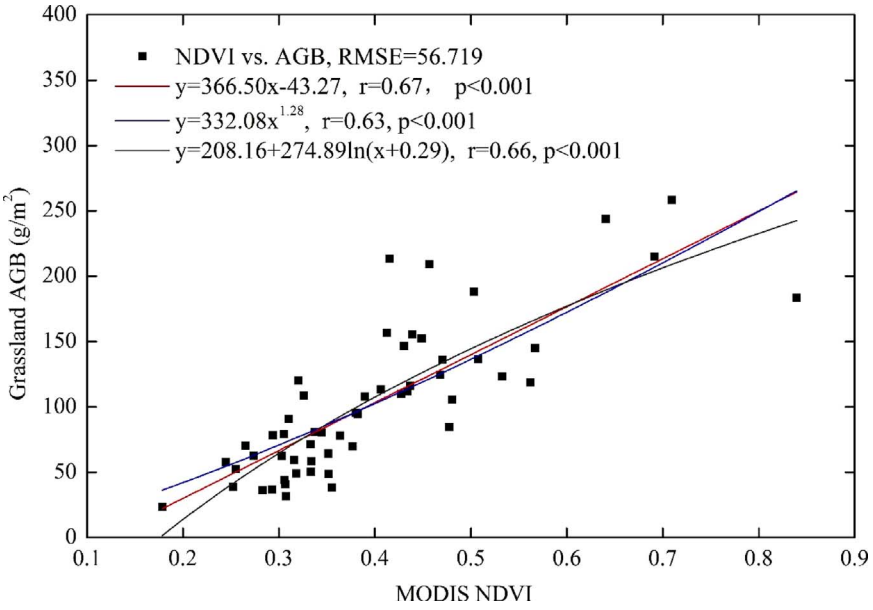

Fig. 2. Relationship of observed AGB and MODSI-NDVI on site level in August 2016.

calculated to evaluate the reversion model for AGB based on MODIS-NDVI. Finally, the reversion model with the best simulation ability was used to characterize the variations in grassland AGB in the growing season during 2005–2015.

As shown in Fig. 2, there was a strong positive correlation between AGB and NDVI at a site scale. Over the study area, the performance of the linear model (r = 0.67) was slightly better than those of the other two models (r = 0.66 for logarithmic model, r = 0.63 for power model), but all the relationships were statistically significant at the 99% confidence level. Generally, there were not large differences among the three models. To avoid over-fitting, we verified the validity of the models for estimating grassland AGB by calculating the parameters of r, RMSE and RE using the validation dataset (Table 2). The results showed that the r value was higher for the linear model (0.65) than for the power model (0.48) and the logarithmic model (0.55). The RMSE value was lower in the linear model (41.58 g/m^2) than in the power model (63.62 g/m^2) and the logarithmic model (51.74 g/m^2). Among the three models, the linear model had the lowest RE. The linear relationship was statistically significant at the 95% confidence level. In addition, this model showed a degree of portability based on the validation for two periods in two neighboring regions. Therefore, the NDVI-AGB linear model showed good performance and was a practical technique to predict grassland AGB accurately for this study area.

2.7. Estimation of potential evapotranspiration (PET)

Potential evapotranspiration (PET) refers to the maximum evaporation of land surface when water supply is not limited under certain meteorological conditions (FAO, 1998). In this study, the revised Penman-Monteith equation given by the world food and Agriculture Organization (FAO) in 1998 is adopted to estimate PET in study area (Bai et al., 2011). The PET was calculated as follows:

Table 2
Performance of three models in estimating grassland AGB based on MODIS-NDVI.

Functional form	r	RMSE (g/m^2)	RE
y = 366.5x − 43.267	0.65	41.58	16.7%
y = 332.078x$^{1.283}$	0.48	63.62	23.9%
y = 274.89ln(x + 0.29) + 251.55	0.55	51.74	19.1%

$$PET = \frac{0.408\Delta(R_n - G) + \gamma\frac{900}{T_{mean}+273}U_2\cdot(VP_s - VP)}{\Delta + \gamma(1 + 0.34U_2)} \quad (10)$$

where *PET* is the potential evapotranspiration, mm/d; R_n is net radiation, $MJ/(m^2\cdot d)$; G is the soil heat flux, $MJ/(m^2\cdot d)$; γ ; Δ is the slope of saturated water vapor pressure, KP$_a$/°C; $U_2$is wind speed at 2 m height, m/s; VP_s is mean saturated vapor pressure, KP$_a$; *VP* is actual saturated vapor pressure, KP$_a$; T_{mean} is mean temperature, °C. Detailed calculations refers to relevant studies (FAO, 1998; Gong et al., 2006).

3. Results

3.1. Changes in species composition over the past 30 years

There are different types of changes in plant communities, because species composition changes in different directions and on different time scales (Chen et al., 2008; Wolf and Toon, 2014). Succession is when one species replaces another, while changes without species succession (smaller changes in species composition) are fluctuations. Therefore, succession occurs on relatively long time scales, and fluctuations occur on shorter time scales. Succession can be regarded as the relationship among structures of plant communities on a temporal scale.

The intensification of desertification inevitably leads to a decrease in species number and diversity. It also changes the dominance of the main species in the community, leading to retrograde succession of the grassland ecosystem. Hence, we focused on analyzing changes in species composition to describe grassland degradation in the last 30 years. The results of this study mainly showed the changes in species composition in meadow grassland in the study area (Fig. 1). We note here that the area was divided into sub-regions on the basis of a species composition map constructed in 1984 that identified areas of grassland with low impact by human activities.

In the map constructed in 1984 (Fig. 3a), there were significant differences in the spatial distribution of species composition, and there was high species richness and diversity. In meadow grassland, the main communities in the west were *L. chinensis; L. chinensis* and *C. squarrosa*; and *L. chinensis, S. baicalensis,* and *C. squarrosa. A Betula platypylla* (*B. platypylla*) and *L. chinensis* community was distributed in the extreme northwest. In the north, the three main communities were *Filifolium sibiricum* (*F. sibiricum*), *S. baicalensis* and *L. chinensis*, and *Pinus sylvestris (P. sylvestris)* and *F. sibiricum*. The northernmost community was *P.*

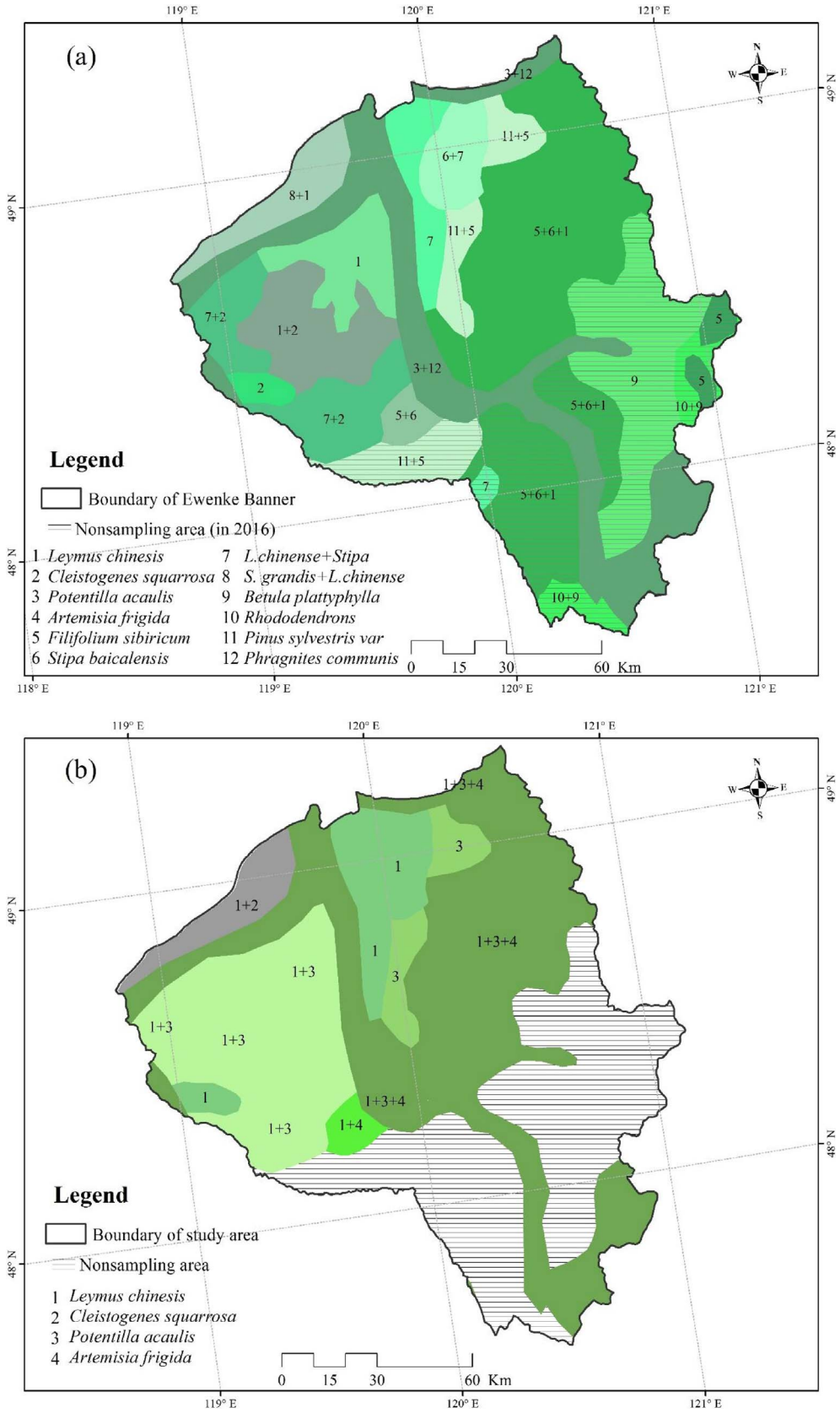

Fig. 3. Species composition mainly in grassland in 1984 (a) compared to 2016 (b).

acaulis and *Phragnites communis* (*P. communis*). Analyses of dominant species composition in 2016 using the SPI method (Fig. 3b) indicated that *L. chinensis* and *P. acaulis* were dominant in the west of this region, *L. chinensis, P. acaulis,* and *A. frigida* were dominant in the north and center, *L. chinensis* and *C. squarrosa* were dominant in the extreme northwest, and *L. chinensis* and *P. acaulis* were dominant species in the remaining areas of the meadow grassland. *A. frigida* and *C. squarrosa* were frequently found as accompanying species.

By comparing species composition between 1984 and 2016, we concluded that species composition had become simpler, but the spatial differentiation of species composition was much less significant. Some components of meadow grassland, such as *F. sibiricum, S. baicalensis*, and *P. sylvestris*, had decreased in abundance or disappeared in 2016. Meanwhile, the abundance of species indicative of grassland degradation including *P. acaulis* and *C. squarrosa* had increased significantly. Communities of *L. chinensis*, and *L. chinensis* and *S. baicalensis* tended to shift to communities of *L. chinensis* and *P. acaulis* at severe stages of degradation. Communities of *F. sibiricum, S. baicalensis* and *L. chinensis,* and of *P. sylvestris* and *F. sibiricum* tended to shift to communities of *L. chinensis, A. frigida,* and *P. acaulis* at moderate stages of degradation. In general, species composition was relatively simpler in 2016 than in 1984, and there was a high proportion of perennial weedy plants including *P. acaulis* and *C. squarrosa*, indicative of grassland degradation. Therefore, the plant community in the semiarid grassland was in the stage of regressive succession.

3.2. Interannual changes in degrees of desertification during 2005–2015

On the basis of the strong correlation between NDVI and vegetation coverage, we assessed the spatial distributions of the degree of desertification (Fig. 4). The spatial distribution of grassland desertification was relatively consistent between 2005 and 2015. The slightly desertified grassland (SlD) grassland was mainly distributed in the west and north, where there was less moderately desertified grassland (MD) and severely desertified grassland (SeD), and non- desertified grassland (non-GD) was distributed in the east and south. These patterns were mainly due to spatial differences in vegetation types (Fig. 1). In 2005, desertification was not a serious problem in the study area, and SlD was the main type of degradation, while MD and SeD were distributed in a narrow zone in the west. And in 2015, the area of SlD had decreased, mainly because it had transformed into non-GD, but the distribution of MD had extended.

Then, we used the transfer matrix method to identify dynamic changes in areas with various degrees of desertification over the study area from 2005 to 2015 (Tables 3 and 4). The proportional area of non-GD was 70.9% higher than those of SlD (27.6%), MD (1.4%), and SeD (0.1%) in 2005. Over the 10 years from 2005 to 2015, SlD showed the largest change (an increase of 23.8% in the total area), followed by non-GD (a decreased of 23.4% in the total area). The changes in the proportional areas of MD and SeD were relatively small. Both exchange variation and net variation occurred mainly in SlD and non-GD. The net variation of non-GD was 21.45%, accounting for 84.5% of total variation in GD. This demonstrated a major decrease in the amount of non-GD, and an increase in the amount of SlD. However, the exchange variation of SeD was roughly equal to its total variation, indicating a shift in spatial position. For MD, exchange variation and net variation were almost equal, indicative of an increase in the amount and a change in spatial position.

Table 3
Desertification transformation matrix in study area in 2015 compared with 2005 (%).

Year	Degree	2015				Total	Decrease
		SeD	MD	SlD	Non-GD		
2005	SeD	0.00	0.05	0.04	0.00	0.09	0.09
	MD	0.03	0.42	0.93	0.03	1.41	0.99
	SlD	0.04	2.42	23.17	1.95	27.57	4.41
	Non-GD	0.01	0.62	22.79	47.50	70.93	**23.43**
Total		0.09	3.51	46.92	49.48	100.00	
Increase		0.09	3.09	**23.76**	1.97		

Table 4
Changes in various degree desertification in study area in 2015 compared with 2005 (%).

	Increase	Decrease	Total variation	Exchange variation	Net variation
SeD	0.09	0.09	0.18	0.18	0.00
MD	3.09	0.99	4.08	1.98	2.10
SlD	23.76	4.41	28.16	**8.81**	19.35
Non-GD	1.97	23.43	25.40	3.95	**21.45**

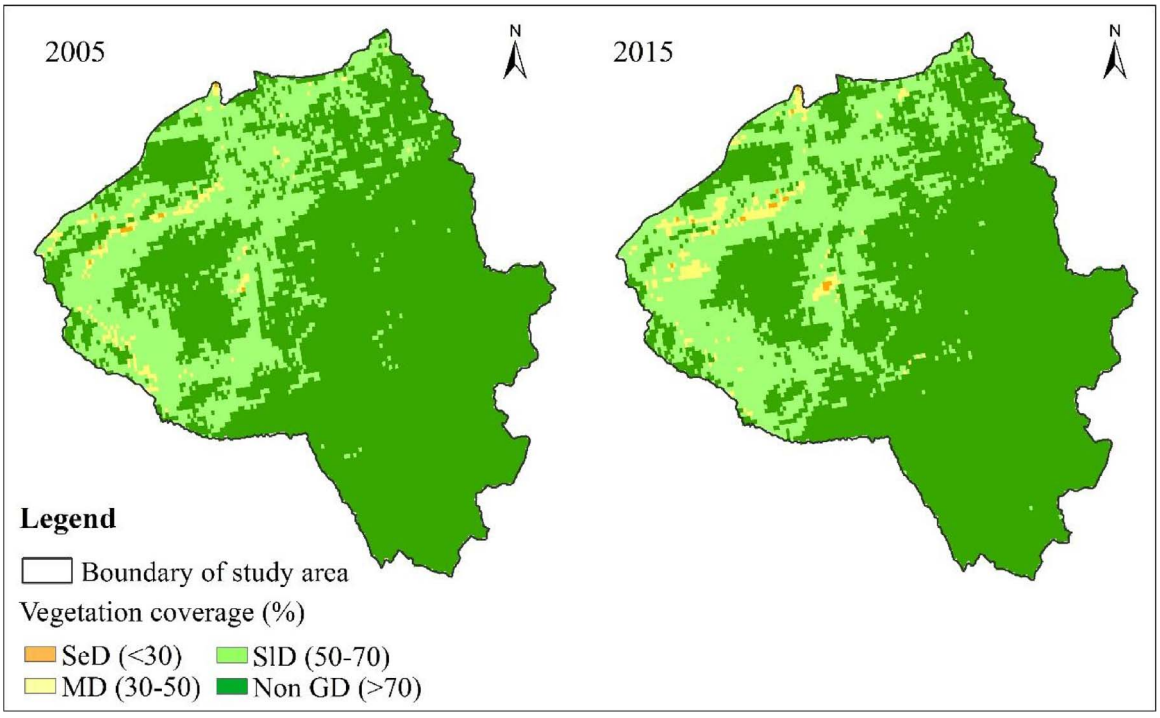

Fig. 4. Spatial distribution of various degrees desertification in August 2005 and 2015.

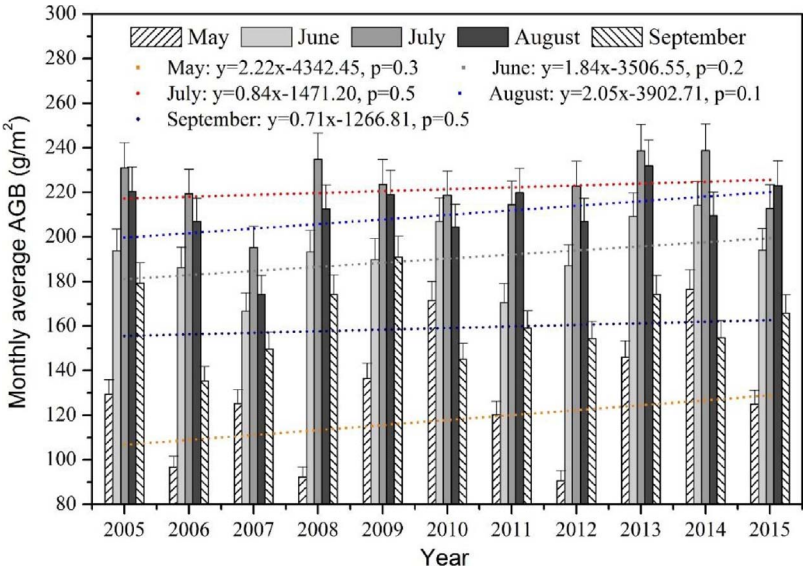

Fig. 5. Predictions of monthly average AGB in growth season over study area from 2005 to 2015.

3.3. Seasonal and interannual characteristics of grassland AGB in the growing season during 2005–2015

The average AGB in each month of the growing season, estimated by the NDVI-AGB linear model, increased slightly in the study area from 2005 to 2015 (Fig. 5). On average, the AGB was highest in July (222.8 g/m^2) and August (221.7 g/m^2), then reduced in September (162.0 g/m^2). The average increase in AGB was largest in May (22.2 g/m^2 per decade), followed by August (20.5 g/m^2 per decade), and was smaller in July and September (8.4 and 7.1 g/m^2 per decade, respectively). Thus, grassland AGB in the growing season increased across the whole region from 2005 to 2015, especially at the beginning of the growing season.

The spatial distribution of average AGB in the growing season from 2005 to 2015 is shown in Fig. 6. There was a gradual increase in average AGB from the northwest to the southeast. Generally, areas where the average AGB in the growing season was less than 200 g/m^2 were mainly in the west and north. Areas with an average AGB greater than 200 g/m^2 and less than 250 g/m^2 were mainly located in the south and east where forest was the main vegetation type. Notably, areas with an average AGB of less than 100 g/m^2 were distributed along a band in the northeast-southwest direction (Fig. 6a). As shown in Fig. 6b, areas showing a decrease in average AGB in the growing season were located in the east and south (decrease of 20 g/m^2 per decade). In the west and north, however, average AGB in the growing season increased at < 20 g/m^2 per decade or from 20 to 50 g/m^2 per decade. Areas where the AGB decreased at > 20 g/m^2 per decade or increased at > 50 g/m^2 per decade were distributed in relatively small areas.

4. Discussion

4.1. Driving climatic factors of change in species composition

Over the past 30 years, there has been a clear trend towards simpler communities with a decrease in species number and diversity from 1984 to 2016. These changes indicated the degradation of the grassland. Research on identifying the driving factors of grassland degradation in semiarid regions has been carried out which suggested grassland degradation results from the combined effects of various environmental factors (e.g., temperature, precipitation etc.) (Yanagawa et al., 2016; Zou et al., 2003; Li et al., 2015). In this study, we analyzed the regional climatic factors (precipitation and temperature) contributing to grassland degradation. We analyzed variations in precipitation and temperature from 1980 to 2015 to coincide with the species composition study period (Fig. 7). Over this period, the average temperature increased (by 0.32 °C/decade) and the average annual precipitation decreased (by 8.9 mm/decade) in the study region ($p < 0.05$). The average annual precipitation ranged from 320.7 to 440.5 mm showing the west grassland became hotter and drier.

The coupling effects of hydrothermal factors determined whether water stress affected the plant community composition and ecosystem productivity. From 1980–2015, precipitation tended to decrease while temperature increased, and so the climate became warmer and drier. The increase in the average temperature increased evapotranspiration from grassland vegetation, consuming more soil water derived from precipitation. Decreased precipitation and increased evapotranspiration seriously restricted vegetation growth, leading to a decrease in species number and diversity. Therefore, the combined effects of water and heat stress over a long time have intensified grassland degradation in the study area.

4.2. Driving climatic factors of changes in desertification and grassland AGB

Based on results of variations of desertification and grassland AGB during 2005–2015, better hydrothermal conditions with increased precipitation, decreased temperature and decreased PET were suitable for grassland growth, therefore there was an increasing trend in average AGB in the growing season overall (Figs. 5 and 8). Analyses of the temporal anomalies in average precipitation, average temperature, and average PET in the growing season from 2005 to 2015 revealed a significant increase ($p < 0.05$) in precipitation in the study area of 193 mm per decade. Average temperature decreased at a rate of 0.9 °C per decade and average PET also slightly decreased at a rate of 0.3 mm per decade. The increase in precipitation and the decreases in temperature and PET became more apparent after 2010 in the study area where the main vegetation type was meadow grassland. These changes in climatic variables in all may partly explain the increasing of AGB during 2005–2015.

However, grassland also had a high sensitivity to climate extremes (Novick et al., 2014; Zhang et al., 2011). Some findings suggested that vegetation growth is influenced by climatic variability in current years, also by its lag effects (Odum et al., 1969). Here, a quantitative way was used to assess the lag effect of climate on vegetation growth (i.e., AGB). As seen from Figs. 5 and 8, interannual variations in precipitation and temperature were adequate to explain AGB variability. Precipitation, the supply source of soil moisture, was the main factor driving the annual variations of grassland growth, even carbon fluxes at the

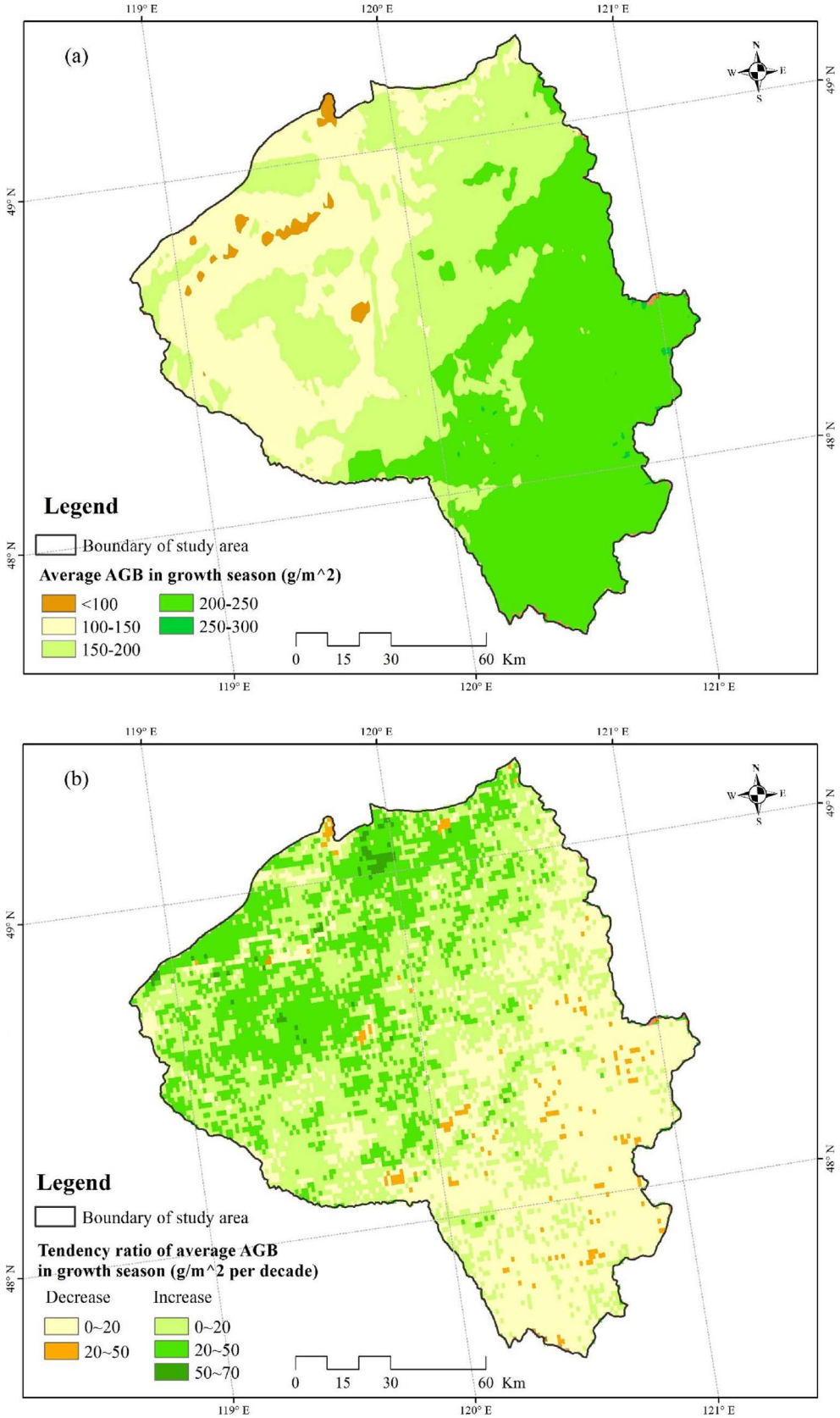

Fig. 6. Spatial distribution of average AGB (a) and its tendency ratio (b) in growth season from 2005 to 2015.

semiarid grassland. Empirical evidences suggested that environmental factors directly caused changes in ecosystem function and structure (Zhang et al., 2015), while few studies had focused on the lag effect on long time scales (Marcolla et al., 2011; Katul et al., 2001). Thus, vegetation growth variability was directly influenced by precipitation and temperature on a short-term scale. However, long-term water-limited conditions, e.g., the period from 2005 to 2010, degraded grassland and accelerated the crisis from grassland to desertification

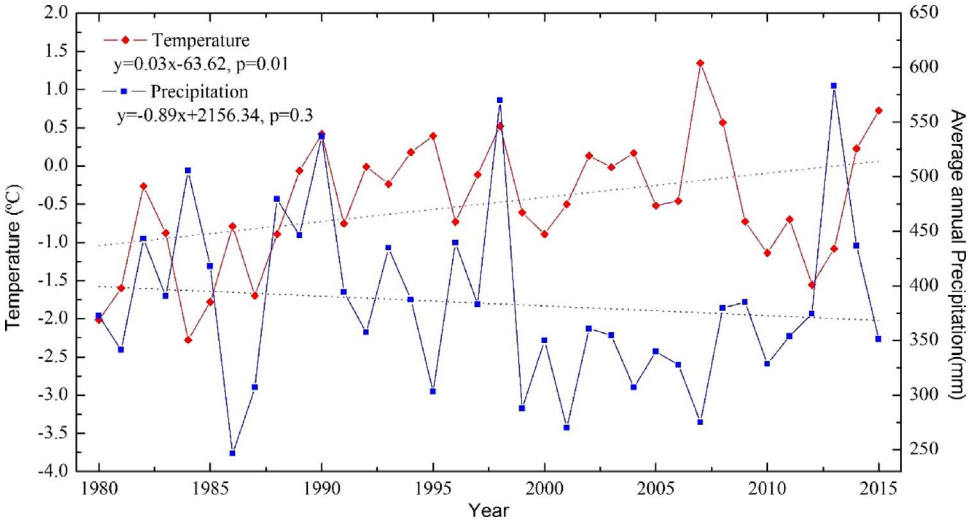

Fig. 7. Temporal distribution of average annual precipitation and average temperature from 1980 to 2015.

gradually. Therefore, our findings suggested that only the two indicators, i.e., grassland AGB and desertification, were fail to reflect grassland degradation or recovery which was consistent with the findings of other studies (Jiang et al., 2010; Li et al., 2016), evolution of species composition indicating community succession of ecosystem must be considered.

4.3. Main limitations and uncertainties

Although this study represents extensive analyses of grassland degradation from multiple perspectives, it has some shortcomings. Firstly, the *in situ* sampling experiments focused on grasslands, and so forest areas were not analyzed. Thus, the NDVI-AGB model to estimate aboveground biomass (AGB) might not be applicable in forest areas. Secondly, we did not record whether the number of mature individuals decreased as the AGB increased, as has been reported elsewhere (Tilman and Downing, 1994). As for the causes of grassland degradation, the latest research indicates that interactions between climatic factors and topographic factors result in spatial differences in vegetation types in different areas (Fuhlendorf et al., 2008; Aguado-Santacruz, 2011). Aguado-Santacruz in 2011 reported a close relationship between the aggregate of several driving factors and grassland degradation. In future research, we intend to carry out a systematic analysis of multiple influential factors using various statistical methods (including principal component analysis) to identify the dominant factors driving grassland degradation.

4.4. Main policy and management

The protection strategies needed are urgent for range expansion of grassland degradation. According to our results and historical findings, human activities and climate change are the main factors leading to grassland degradation. Thus, the managements of grassland degraded by different drivers should be provided. Human intervention measures, including fencing and enclosures, low intensity grazing, prohibition for native grassland reclaimation, etc., should be considered. However, for degradation due to climate change, some drying, drought- and cold-resistent species should be introduced to reduce the interference of hydroclimatic disturbances on the grassland.

5. Conclusions

Our results indicated that three indicators of grassland degradation (species composition, desertification, and AGB) gave inconsistent estimates of grassland degradation in the study area on different time scales. Over the past 30 years, an increase in average temperature and a decrease in average precipitation have led to a simplification of plant communities, with lower species number and diversity in 2016 than in 1984. During the period from 2005 to 2015, the decrease in average temperature and average PET and increase in average precipitation

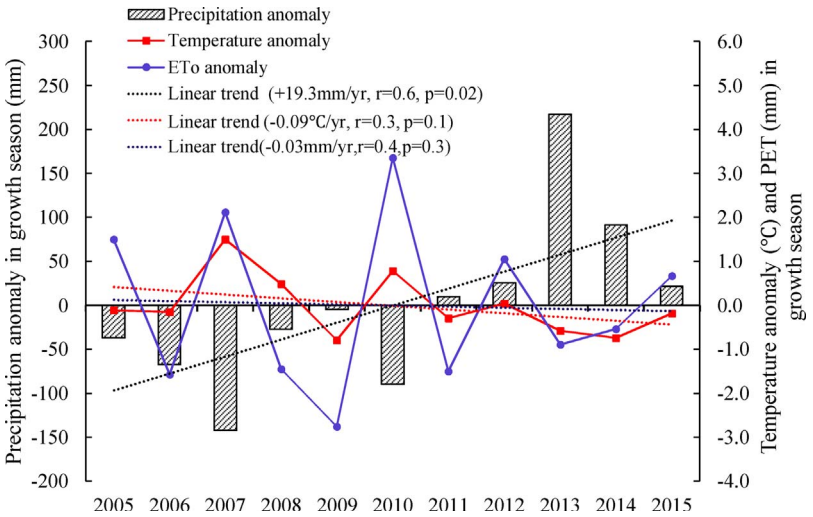
Precipitation anomaly
Temperature anomaly
ETo anomaly
Linear trend (+19.3mm/yr, r=0.6, p=0.02)
Linear trend (-0.09°C/yr, r=0.3, p=0.1)
Linear trend(-0.03mm/yr,r=0.4,p=0.3)
Precipitation anomaly in growth season (mm)
Temperature anomaly (°C) and PET (mm) in growth season

Fig. 8. Interannual variations in anomalies of precipitation, temperature and ETo in growth season from 2005 to 2015.

relieved grassland desertification and promoted grassland growth. Owing to spatial differences in temperature and precipitation, the degree of desertification shifted from non-GD to SlD, especially in the west. In conclusion, *in situ* investigations and dataset analyses to compare species composition between different times showed that grassland in the study area has seriously degraded. Analyses of desertification and grassland AGB on a shorter time scale indicated that the grassland ecosystem was recovering, whereas analyses of species composition indicated that the grassland ecosystem was degrading. Thus, multiple perspectives should be considered to define grassland degradation. Various indicators and different time scales should be considered to draw accurate conclusions about the state of ecosystems. Results in this study can provide an appropriate strategy for grassland restoration and management, making a contribution to sustainable regional socioeconomic development.

Acknowledgements

This study was supported by the National Natural Science Foundation of China (Grant No. 51679006) and the Evaluation of Resources-Environmental Carrying Capacity in Typical Ecological Zones of Xinganling (Grant No. 12120115051201).

References

Aguado-Santacruz, G.A., 2011. Development of long-term and reliable in vitro plant regeneration systems for elite malting barley varieties: optimizing media formulation and explant selection. Afr. J. Biotechnol. 10, 19522–19533.
Amarnath, G., Babar, S., Murthy, M.S.R., 2017. Evaluating MODIS-vegetation continuous field products to assess tree cover change and forest fragmentation in India – a multi-scale satellite remote sensing approach. Egypt. J. Remote Sens. Space Sci. 20, 157–168.
Bai, M., Hao, R., Hou, Q., Di, R., Yang, J., 2011. Impact of climatic vacillation on potential evaporation on typical grassland. Trans. Atmos. Sci. 34, 351–355.
Carroll, M., Townshend, J., Hansen, M., Dimiceli, C., Sohlberg, R., Wurster, K., 2010. MODIS Vegetative Cover Conversion and Vegetation Continuous Fields. Springer, New York.
Chen, T., Liu, X.N., Xin, X.P., Zhand, X., Yuan, L., 2008. The relationship between community species diversity and degradation degree of Leymus chinensis meadow steppe in the Hulunbeier. J. Gansu Agric. Univ. 43, 135–141.
Coyle, D.R.C.R., Colemancoleman, M.D., Aubrey, D.P.A.P., 2008. Above- and below-ground biomass accumulation, production, and distribution of sweetgum and loblolly pine grown with irrigation and fertilization. Can. J. For. Res. 38 (38), 1335–1348.
Food and Agriculture Organization of the United Nations, 1998. Crop Evapotranspiration: Guidelines for Computing Crop Requirements. Food & Agriculture Org., Italy.
Fuhlendorf, S.D., Archer, S.A., Smeins, F., Engle, D.M., Taylor, C.A., 2008. The combined influence of grazing, fire, and herbaceous productivity on tree–grass interactions. West. North Am. Juniperus Commun. 219–238.
Gong, L., Xu, C.Y., Chen, D., Halldin, S., Chen, Y.D., 2006. Sensitivity of the Penman–Monteith reference evapotranspiration to key climatic variables in the Changjiang (Yangtze River) basin. J. Hydrol. 329 (3), 620–629.
He, X.D., 2004. Amending of importance value and its application on classification of Leymus chinensis communities. Bull. Bot. Res. 24, 466–472.
Holben, B., 1986. Characteristics of maximum-value composite images from temporal AVHRR data. Int. J. Remote Sens. 7 (11), 1417–1434.
Huo, A.D., Zhang, G.J., Wu, S.L., Yue, M., 2008. The application of remote sensing technique to sandy desertification assessment based on MODIS data-Taking North Shaanxi as an example. Agric. Res. Arid Areas 26 (2), 154–158.
Jiang, Y., Bi, X.L., Huang, J.H., Bai, Y.F., 2010. Patterns and drivers of vegetation degradation in xilin river basin, inner Mongolia, China. Chin. J. Plant Ecol. 34 (10), 1132–1141.
Kang, L., Han, X., Zhang, Z., Sun, O.J., 2007. Grassland ecosystems in China: review of current knowledge and research advancement. Philos. Trans. R. Soc. Lond. 362 (1482), 997.
Katul, G., Lai, C.T., Schäfer, K., Vidakovic, B., Albertson, J., Ellsworth, D., Oren, R., 2001. Multiscale analysis of vegetation surface fluxes: from seconds to years. Adv. Water Resour. 24, 1119–1132.
Li, J., Jian, W., 2004. Estimating plant biomass in jun ma chang of shandan county using landsat TM data. Remote Sens. Technol. Appl. 19 (5), 343–347.
Li, S.Y., Li, X.B., Ying, G., Fu, N., 2007. Vegetation indexes biomass models for typical semiarid steppe-A case study for Xilinhot in Northern China. Chin. J. Plant Ecol. 31 (1), 23–31.
Li, Z.H., Bao, Y.J., Zhang, J., Wang, H.M., HU, Z.C., 2015. Comparative analysis on degradation and its driving factors in xilin gol grassland and hulun buir grassland. J. Dalian Nationalities Univ. 17, 1–5.
Li, Y.J., Cao, G.M., Long, R.J., Yao, T., 2016. Effects of land use patterns on grassland biomass and soil properties in three-river headwater area. Acta Agrestia Sin. 3 (24), 524–529.
Man, J., Deng, B., Zhang, J.L., Li, J.H., Li, D.Q., Liu, J., 2016. Effects of litter covering on typical grassland vegetation and soil characteristics in inner Mongolia. Chin. J. Grassland 38 (2), 59–64.
Marcolla, B., Cescatti, A., Manca, G., Zorer, R., Cavagna, M., Fiora, A., Gianelle, D., Rodeghiero, M., Sottocornola, M., Zampedri, R., 2011. Climatic controls and ecosystem responses drive the inter-annual variability of the net ecosystem exchange of an alpine meadow. Agric. For. Meteorol. 151, 1233–1243.
Novick, L.R., Schreiber, E.G., Catley, K.M., 2014. Deconstructing evolution education: the relationship between micro- and macroevolution. J. Res. Sci. Teach. 51, 759–788.
Odum, W.E., Woodwell, G.M., Wurster, C.F., 1969. DDT residues absorbed from organic detritus by fiddler crabs. Science 164, 576–577.
Peng, H.Y., Li, X.Y., Tong, S.Y., 2013. Effects of shrub encroachment on biomass and biodiversity in the typical steppe of Inner Mongolia. Acta Ecol. Sin. 33 (22), 7221–7229.
Qin, Z., Zhu, Y., Li, W., Xu, B., 2008. Mapping vegetation cover of grassland ecosystem for desertification monitoring in Hulun Buir of Inner Mongolia, China. Proc. SPIE Int. Soc. Opt. Eng. 7104.
Ren, J.Z., 1998. Grassland Science Research Methods. Agriculture Press, Beijing: China, pp. 36.
Sarula, Hou, X.Y., Li, J.X., Ding, Y., Wu, X.H., Yun, X.J., 2013. Organic carbon storage in vegetation-soil systems of typical grazing degraded steppes. Acta Pratacult. Sin. 22 (5), 18–26.
Tilman, D., Downing, J.A., 1994. Biodiversity and stabilty in grasslands. Nature 6461 (367), 363–365.
Todd, S.W., Hoffer, R.M., Milchunas, D.G., 1998. Biomass estimation on grazed and ungrazed rangelands using spectral indices. Int. J. Remote Sens. 19 (3), 427–438.
Wang, X., Guo, Y., He, J., 2014. Estimation of above-ground biomass of grassland based on multi-source remote sensing data. Trans. Chin. Soc. Agric. Eng. 30 (11), 159–166.
Wang, P., Lassoie, J.P., Morreale, S.J., Dong, S., 2015. A critical review of socioeconomic and natural factors in ecological degradation on the Qinghai-Tibetan Plateau, China. Rangeland J. 37 (1).
Wang, Z., Deng, X., Song, W., Li, Z., Chen, J., 2017. What is the main cause of grassland degradation? A case study of grassland ecosystem service in the middle-south Inner Mongolia. Catena 150, 100–107.
Wolf, E.T., Toon, O.B., 2014. Controls on the Archean climate system investigated with a global climate model. Astrobiology 14, 241.
Wu, X., Li, Z.S., Fu, B.J., Lu, F., Wang, D.B., Liu, H.F., 2014. Effects of grazing exclusion on soil carbon and nitrogen storage in semi-arid grassland in inner Mongolia, China. Chine. Geogr. Sci. 24 (4), 479–487.
Yanagawa, A., Sasaki, T., Jamsran, U., Okuro, T., Takeuchi, K., 2016. Factors limiting vegetation recovery processes after cessation of cropping in a semiarid grassland in Mongolia. J. Arid Environ. 131, 1–5.
Zhang, G., Xingliang, X.U., Zhou, C., Zhang, H., Hua, O., 2011. Responses of vegetation changes to climatic variations in hulun buir grassland in past 30 years. Acta Geogr. Sin. 1 (66), 47–58.
Zhang, T., Xu, M., Xi, Y., Zhu, J., Tian, L., Zhang, X., Wang, Y., Li, Y., Shi, P., Yu, G., Sun, X., Zhang, Y., 2015. Laggedclimatic effects on carbon fluxes over three grassland ecosystems in China. J. Plant Ecol. 8, 291–302.
Zhao, H., Liu, S., Dong, S., Su, X., Wang, X., Wu, X., 2015. Analysis of vegetation change associated with human disturbance using modis data on the rangelands of the qinghai-tibet plateau. Rangeland J. 1 (37), 77.
Zou, Y.R., Zhang, Z.X., Zhou, Q.B., Zhao, X.L., Liu, B., 2003. Spatial pattern and its analysis of China's grassland change in recent ten years using remote sensing and GIS. J. Remote Sens. 428–432.